Second Workshop on Integration of EFD and CFD
24th Feb 2009, JAXA

Static Aeroelasticity Analyisis of AGARD-B Wind Tunnel Calibration Model Using Discontinuous Galerkin CFD Solver

Kanako YASUE*
and
Keisuke SAWADA

* Ph.D Student, Graduate School of Engineering,
Dept. of Aerospace Engineering, Tohoku University, JAPAN

Prediction of Aerodynamic Characteristic

- Accurate prediction of aerodynamic characteristics
  - Affected by boundary layer transition and separation
  - Required wind tunnel test with actual flight Re number
- Conventional wind tunnel test
  - 1 or 2 order lower Re number compared with actual flight due to model size restriction or facility restriction
  - Putting roughness to promote turbulent transition at lower Re number
  - Extrapolation of the aerodynamic performance in actual flight from wind tunnel data (Re number scaling effect)

High Re Number Wind Tunnels

- National Transonic Facility (US, 1982)
- European Transonic Wind-tunnel (Germany, 1993)
  - High Re number comparable to that of actual flight environment
  - Lowering temperature of pressurized airflow to that of cryogenic level

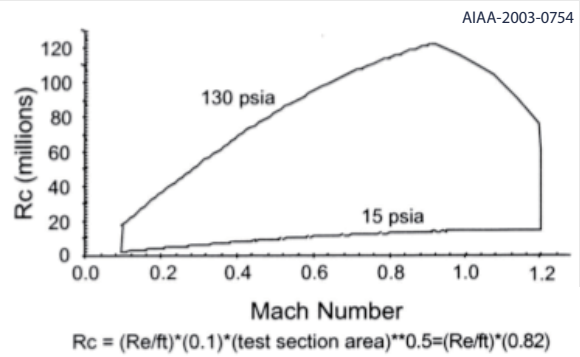

NTF performance envelope

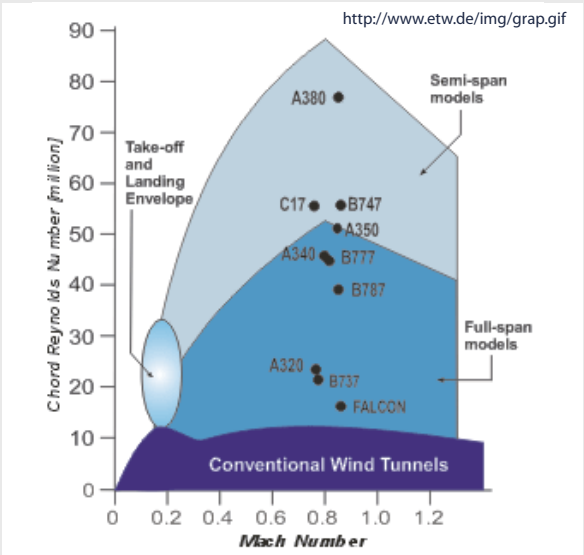

ETW performance envelope

03

Features of High Re Number Wind Tunnel

- Highly pressurized airflow
- Larger aerodynamic load on the model
- Model deformation of thin part
- Altering aerodynamic features
- Masking Re number scaling effect

In NTF and ETW

- Independent control of total pressure and total temperature
- Separate evaluation of Re number effect and model deformation effect

04

High Re Number Wind Tunnel in Japan

- Trisonic Wind Tunnel (Japan, 2005)
  - Highly pressurized airflow (P_{0max}=1.4 MPa, Re_{max}=1x10^8 /m)
  - Cannot control total pressure and total temperature independently
  - Cannot isolate Re number scaling effect and model deformation effect

Accurate prediction of aerodynamic performance in TWT

- Isolation of model deformation effect using CFD
- Small change in geometry of wind tunnel model causes small change in aerodynamic performance

  ⇒ High-order CFD schemes

05

Objectives

- Explore effect of model deformation in TWT by fluid-structure interaction analysis
  - Static aeroelasticity analysis of AGARD-B wind tunnel calibration model
    - CFD analysis : Discontinuous Galerkin (DG) method

      ⇒High order spatial accuracy on unstructured mesh
    - Structural analysis : NX/NASTRAN®
  - Examination of model deformation and its influence to aerodynamic characteristics

06

Discontinuous Galerkin Method

$$\iiint_{\Omega} w(\mathbf{x}) \left(\frac{\partial Q}{\partial t} + \nabla \cdot \mathbf{F}(Q) \right) d\Omega = 0$$

$$Q(\mathbf{x},t) = \sum_j Q_j(t) v_j(\mathbf{x})$$

$$w(\mathbf{x}) \leftarrow v_i(\mathbf{x})$$

$w(\mathbf{x})$: test function

$Q_j(t)$: degree-of-freedom (DOF)

$v_j(\mathbf{x})$: basis function (Jacobi polynomial)

$$\sum_j \frac{dQ_j}{dt} \iiint_{\Omega} v_i v_j d\Omega + \iint_{\partial\Omega} v_i \mathbf{F}(Q) \cdot \mathbf{n} d\sigma - \iiint_{\Omega} \mathbf{F}(Q) \cdot \nabla v_i d\Omega = 0$$

- Basis functions and dependent variables become discontinuous at cell interface
- Numerical flux is given by approximate Riemann solver
- Viscous term is discretized using BR2 formulation

Pointwise Relaxation Implicit Scheme

- Flux function is solely expanded by the change of DOFs in own computational cell
- Resulting algebraic equation is pointwise

$$\mathbf{F}^{n+1} \cong \mathbf{F}^n + \frac{\partial \mathbf{F}^n}{\partial Q} \Delta Q = \mathbf{F}^n + \frac{\partial \mathbf{F}^n}{\partial Q} \sum_j v_j \Delta Q_j$$

$$\sum_j \frac{dQ_j}{dt} \int_{\Omega} v_i v_j d\Omega + \int_{\partial\Omega} v_i \mathbf{F}^{n+1}(Q_h) \cdot \mathbf{n} d\sigma - \int_{\Omega} \mathbf{F}^{n+1}(Q_h) \cdot \nabla v_i d\Omega = 0$$

$$\mathcal{M}^n \Delta Q_j = \mathcal{R}^n$$

size of $\mathcal{M}^n$ = [(# of Dependent variables)×(# of DOFs)]^2

$$\mathcal{M}^n = \frac{1}{\Delta t} \sum_j \int_{\Omega} v_i v_j d\Omega + \sum_j \int_{\partial\Omega} v_i \left(\frac{\partial \mathbf{F}^n}{\partial Q} \cdot \mathbf{n} \right)^+ v_j d\sigma - \sum_j \int_{\Omega} v_i \left(\frac{\partial \mathbf{F}^n}{\partial Q} \nabla v_i \right) v_j d\Omega$$

$$\mathcal{R}^n = - \int_{\partial\Omega} v_i \mathbf{F}^n(Q_h) \cdot \mathbf{n} d\sigma + \int_{\Omega} \mathbf{F}^n(Q_h) \cdot \nabla v_i d\Omega$$

Aeroelasticity Analysis Procedure

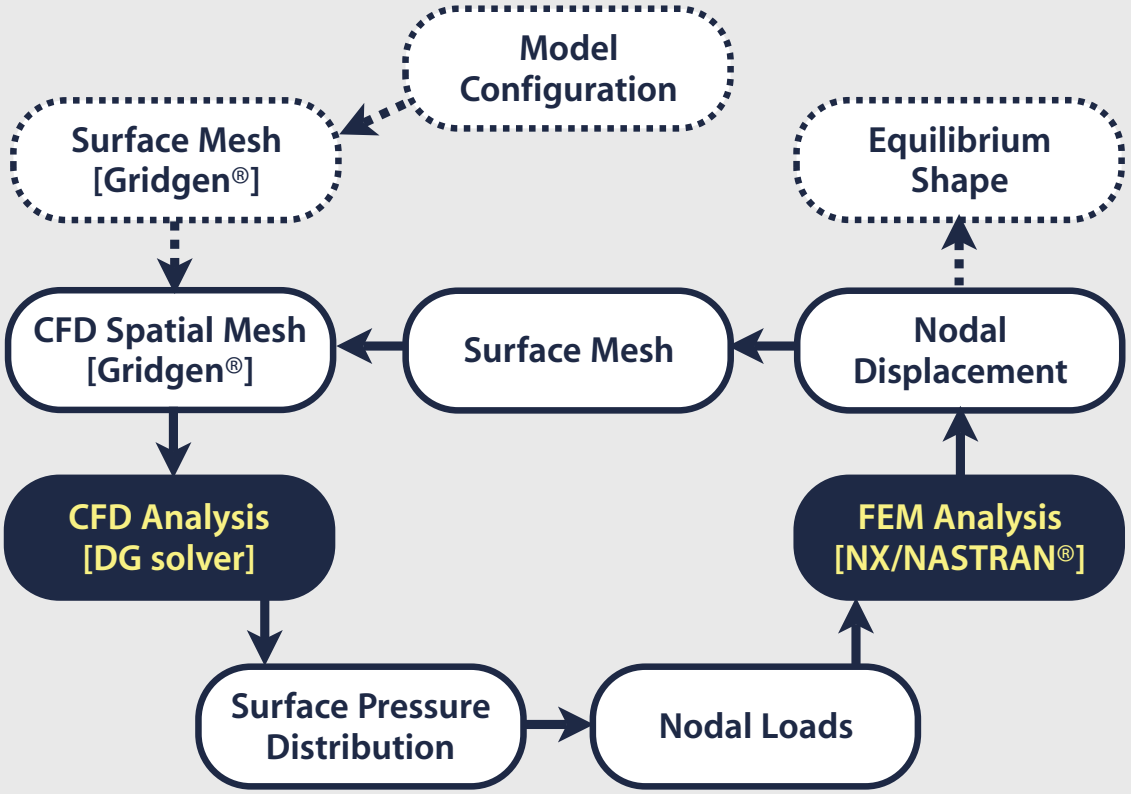

09

Supersonic Flowfield over AGARD-B Model

Numerical Schemes

- RANS equations
- 2nd order DG method
- Pointwise relaxation implicit scheme
- AUSM-DV upwind scheme
- BR2 formulation
- Spalart-Allmaras turbulence model
- Slope limiter
- CFL=10^5

Parallelization

- METIS grid partitioning
- MPI Library
- Xeon Dual Core 3.0GHz x2 (4cores)

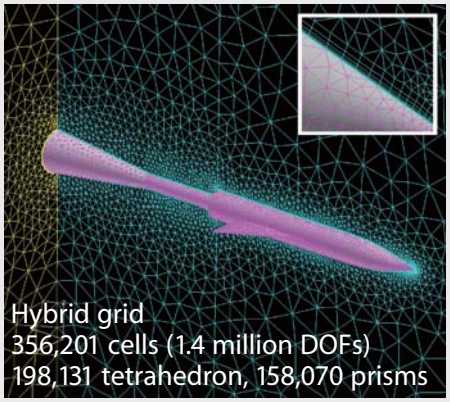

AGARD-B model configuration

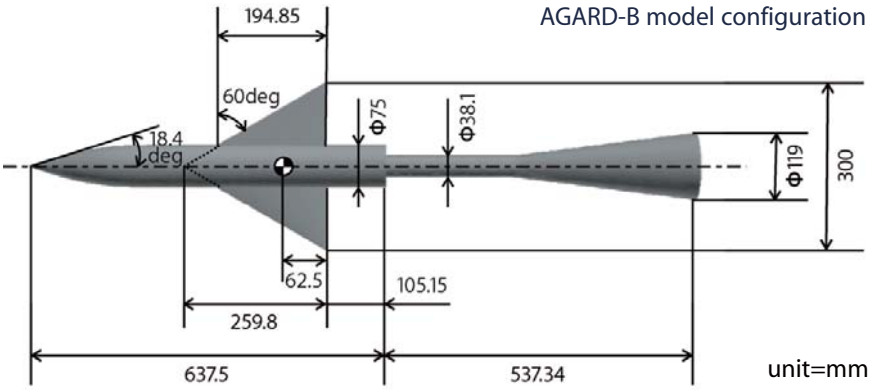

10

Flow Conditions (TWT)

	Mach number	Angle of Attack [deg]	Side Slip Angle [deg]	Re number x10^6 [1/m]	Total Pressure [kPa]	Total Temperature [K]
Case1	1.4	0.098	-0.005	27.6	167.1	276.4
Case2	1.4	4.303	-0.003	27.8	167.0	274.5
Case3	1.4	8.535	-0.001	27.9	167.1	273.9

Pressure and Mach Number Contours

Baseline Computations

Case1 (α=0.09) Case2 (α=4.30) Case3 (α=8.53)

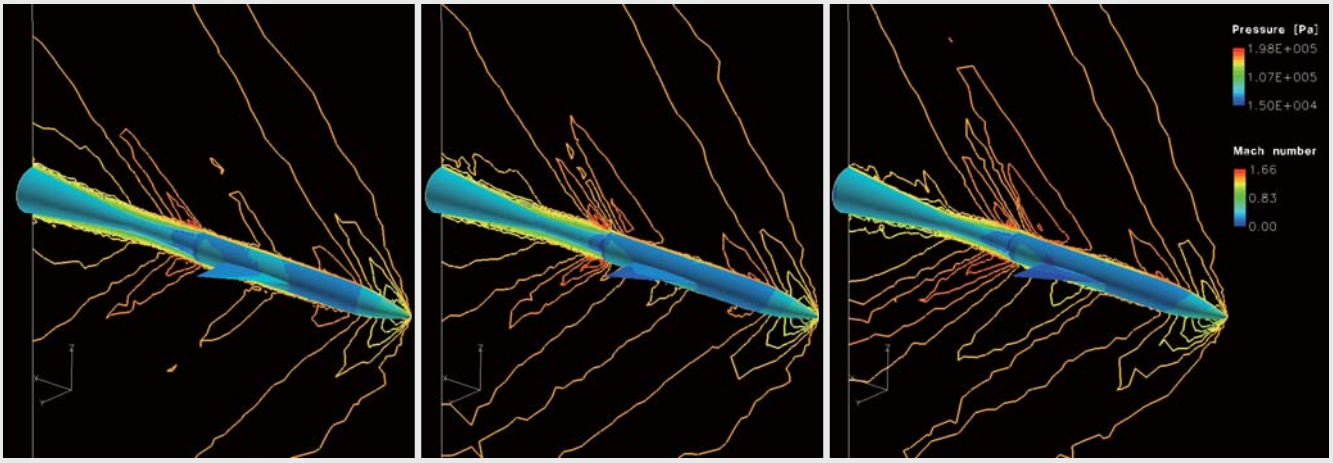

Convergence Histories

Baseline Computations

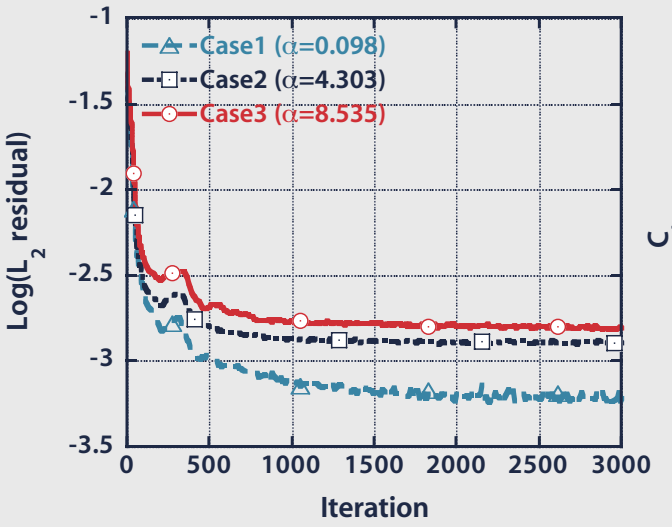

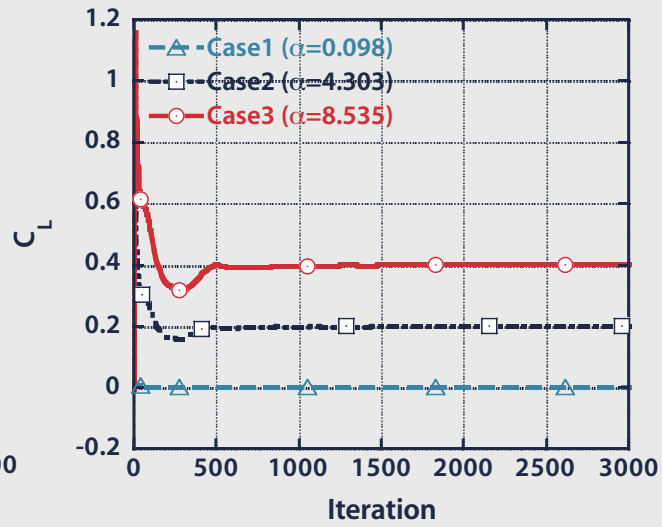

- L_2 residual and C_L are converged within 3000 iterations
- L_2 residual decreases only for 2 orders of magnitude

13

Aerodynamic Coefficients

Baseline Computations

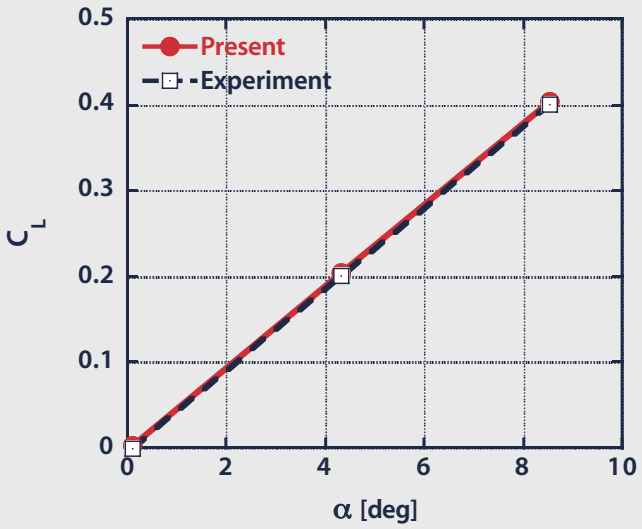

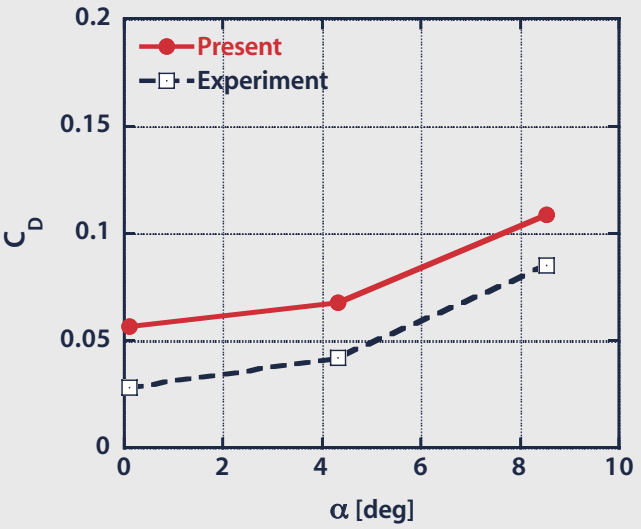

- Using finer mesh and considering effect of turbulence transition at trip location will be needed

14

Aeroelasticity Analysis of AGARD-B Model

Structural computation by NX Nastran

- SUS304
- Same surface mesh with CFD
- Nodal load data converted from steady state CFD solution at surface boundary
- Fixed condition at root plane boundary

Flowfield computation

- RANS equations
- 2nd order DG method
- Pointwise relaxation implicit scheme
- AUSM-DV upwind scheme
- BR2 formuration
- Spalart-Allmaras turbulence model
- Slope limiter
- CFL=10^5

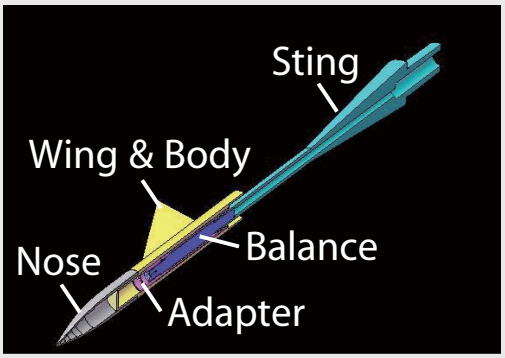

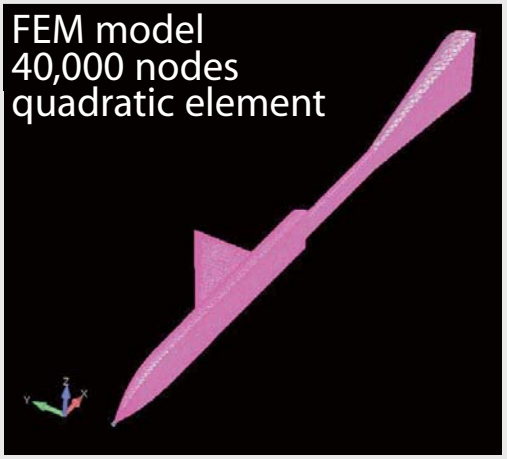

15

Obtained Model Deformation

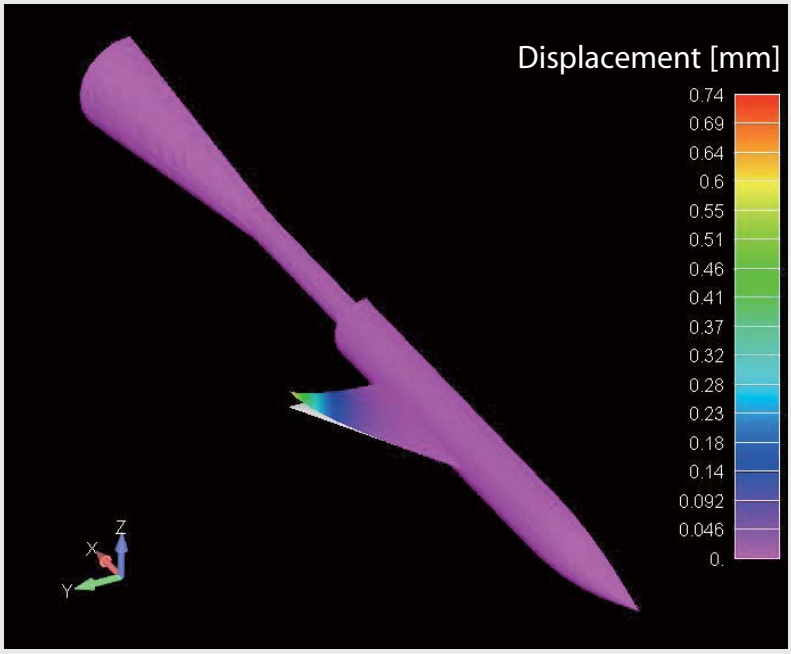

- Model deformation analysis is only considered for Case3 (α=8.5)
- Maximum wing tip displacement is 0.737 mm

16

Converged Deformation along Trailing Edge

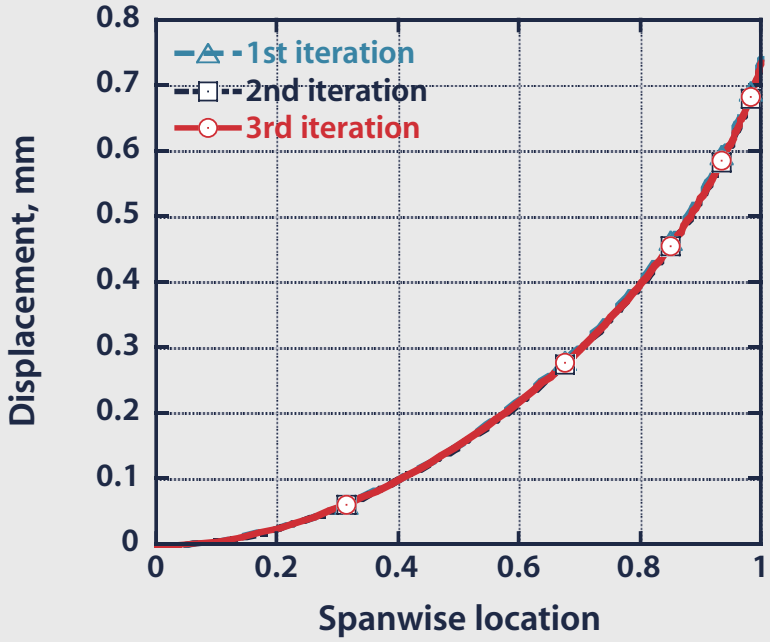

- Convergence is obtained only within 3 iterations in this case

17

Aerodynamic Characteristics

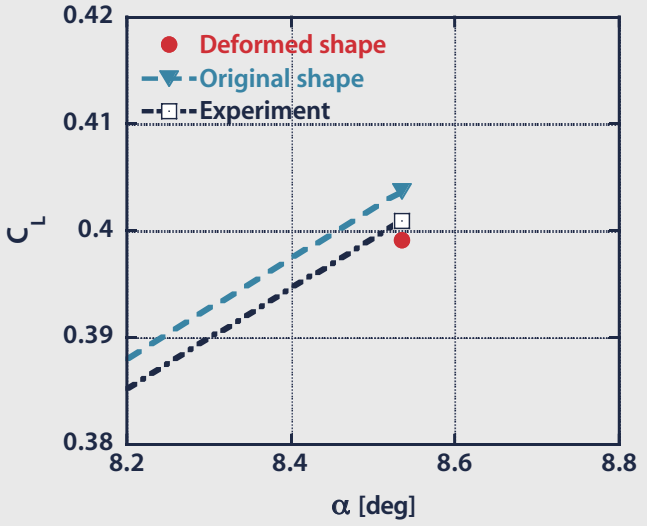

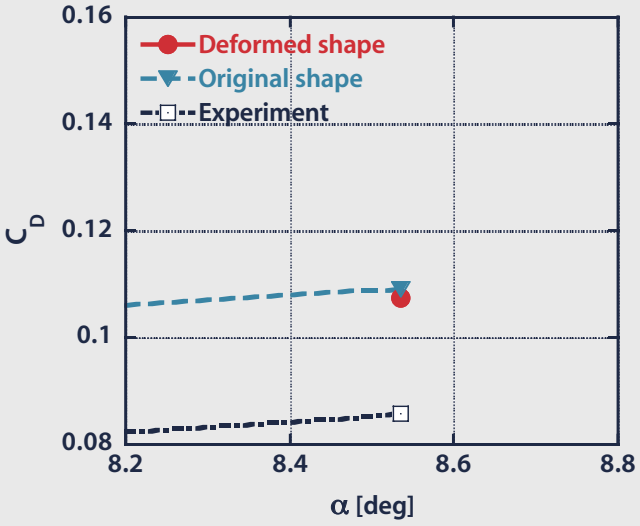

- C_L decreases 0.0047 due to model deformation
- C_D decreases 0.0018 due to model deformation
- Even for small displacement, resulting change in aerodynamic coefficient cannot be ignored

18

Concluding Remarks

- The aeroelasticity analysis of AGARD-B wind tunnel calibration model is successfully carried out
  - Pointwise relaxation implicit discontinuous Galerkin method for flowfield computation is coupled with NX/NASTRAN for structural analysis
  - Maximum deformation of wing tip is less than 1mm
  - ΔC_L and ΔC_D due to model deformation cannot be ignored
  - DG solver is suitable for static aeroelasticity analysis
- Effect of model deformation should be isolated in experimental data of TWT for higher Re number conditions

19

Future Works

- Computation using finer mesh and considering turbulent transition at the trip location
- Higher order approximation and boundary representation for flowfield computation
- Considering internal structure for elasticity analysis
- Constructing techniques to isolate Re number effect and model deformation effect in TWT

20